Radiative Heat Transfer in Falkner's-Skan Flow of a Carreau Fluid Over a Wedge with Non-Uniform Heat Source/Sink

C. Sulochana[1*], A. Sivamma[1,2], G.P. Ashwinkumar[3*]

[1]Department of Mathematics, Gulbarga University, Kalaburagi, Karnataka, India

[2]Department of Mathematics, Rao Bahadur Y Mahabaleswarappa Engineering College, Ballari, India

[3]Department of Mathematics, Vijayanagara Sri Krishnadevaraya University, Ballari, Karnataka, India

DOI: https://doi.org/10.51244/IJRSI.2026.13010189

Received: 21 January 2026; Accepted: 28 January 2026; Published: 14 February 2026

ABSTRACT

This study focuses on radiative heat transfer in Falkner-Skan flow of a Carreau fluid influenced by a wedge surface in the presence of non-uniform heat source/sink. The governing nonlinear partial differential equations (PDE's) are reduced to a system of nonlinear ordinary differential equations (ODE's) using similarity transformations. These ODE's are numerically solved using the bvp5c MATLAB package, yielding detailed insights into the velocity and temperature distributions. The analysis highlights the effects of critical parameters, including the Carreau fluid properties, radiation, wedge angle, and non-uniform heat source/sink, on the flow and thermal behaviour. A comparison benchmark is presented to validate the numerical solutions. This work offers significant contributions to the understanding of heat transfer in non-Newtonian fluid flows, with practical applications in engineering and industrial sectors.

Keywords: Falkner-Skan flow; thermal radiation; non-uniform heat source/sink; Carreau fluid.

INTRODUCTION

In recent years, non-Newtonian fluids have garnered significant attention from researchers due to their extensive applications in engineering and technological processes. The rheological complexity of these fluids arises from their constitutive relationships, which involve higher-order differential systems and diverse flow characteristics. Although numerous models have been proposed to capture the behaviour of non-Newtonian fluids, no single model can comprehensively account for all their properties. Among these, the Carreau fluid model, introduced by Carreau in 1972 [1], stands out for its effectiveness in describing the behaviour of a wide range of non-Newtonian fluids. This model is particularly relevant in addressing polymer processing and lubrication challenges, as it incorporates both shear-thickening and shear-thinning effects through its dependence on the power-law index. The Carreau fluid model accurately characterizes the rheological properties of polymeric solutions, including glycerol containing 0.3% hydroxyethyl-cellulose, 1% methylcellulose tylose, and polyethylene oxide. These polymers play a crucial role in applications like capillary electrophoresis, where they are employed to enhance resolution in DNA and protein separation, as highlighted in the studies by Corradini [2] and Heller [3]. The Carreau fluid model, renowned for its versatility and precision, has established itself as a fundamental tool in rheological research, motivating a wide range of investigations by researchers [4-15].

On the other hand, a steady laminar flow of a viscous fluid passing a fixed wedge with potential flow velocity was first studied by Falkner and Skan [16]. They have used a special type of similarity transformations to convert the partial differential equations into ordinary differential equations. Reduced equations are well known by the name Falkner-Skan equations. There are many of literature on the solutions of Falkner-Skan equations, for instance, see; Hartree [17], Stewartson [18], Chen and Libby [19], Botta et al. [20], Brodie and Banks [21] and Kuo [22]. Recently, Ishak et al. [23] have presented the numerical solutions for two-dimensional Falkner-Skan flows over a moving wedge by utilizing non-Newtonian fluid. Yacob et al. [24] have studied the Falkner-Skan problem for a wedge immersed in nanofluids. To solve the complicated boundary layer problem they have employed Runge-Kutta-Fehlberg method. Yacob et al. [25] have reported the dual solutions for fluid flow and heat transfer over moving wedge through prescribed surface heat flux boundary conditions. Makinde [26] have presented the similarity solution for moving vertical plate in natural convection flow with internal heat generation and the author investigated the convective boundary condition for heat transfer enhancement. The mixed convection flow and radiative heat transfer of viscoelastic fluid over a porous wedge have been investigated by Rashidi et al. [27]. Mustafa [28] investigated the traditional Jeffery-Hamel flow in convergent/divergent channels with channels are stretching or shrinking. Abbasbandy et al. [29] have presented the numerical and analytical solutions for Falkner-Skan flow of MHD Oldroyd-B fluid. Mustafa [30] presented the exact analytical solutions for the Falkner-Skan slip flow and heat transfer of viscous fluid over a wedge. Hayat [31] studied the Falkner-Skan flow of an incompressible Walters-B fluid using the Homotopy Analysis Method (HAM). The fluid flow was induced by a stretching wedge, incorporating thermal radiation and a specified surface heat flux. Chamkha et al. [32] investigated the effects of temperature-dependent viscosity and variable Prandtl number on the forced convective Falkner-Skan flow of Williamson nanofluid.

The influence of thermal radiation significantly affects the rate of heat transfer and the temperature distributions in the boundary layer flow of participating fluid. So, the thermal radiation effect plays an important role in controlling heat transfer in industrial and engineering applications. The mixed convection radiative heat flow over a permeable vertical surface was studied by Bakier [33]. Al-Odat et al. [34] have analysed the impact of thermal radiation on mixed convection fluid flow over a wedge through a non-Darcy porous medium. The effect of mixed convection MHD flow and radiative heat transfer over vertical isothermal surface embedded in a porous medium has been numerically analysed by Damseh [35]. The MHD unsteady flow of a radiating fluid with the effect of chemically reaction and constant heat flux over a vertical plate has been presented by Makinde [36]. Turkyilmazoglu and Pop [37] have investigated the unsteady natural convection flow and radiative heat transfer of nanofluid past a vertical infinite flat plate. In this direction authors [38-42] is utilized to thermal radiation effect to analyse the heat transfer mechanism.

Although there has been considerable research on non-Newtonian fluids, the study of MHD Falkner-Skan flow of Carreau fluid with non-uniform heat source/sink and radiation remains received limited attention. Inspired by the findings from previous studies and their significance in industrial and engineering applications, this paper presents a detailed numerical analysis of the Carreau fluid model. The governing system of nonlinear ordinary differential equations (ODEs) is derived using similarity transformations and solved numerically through the shooting method. The effects of key physical parameters are analysed and presented using both tabular data and graphical representations.

Mathematical formulation

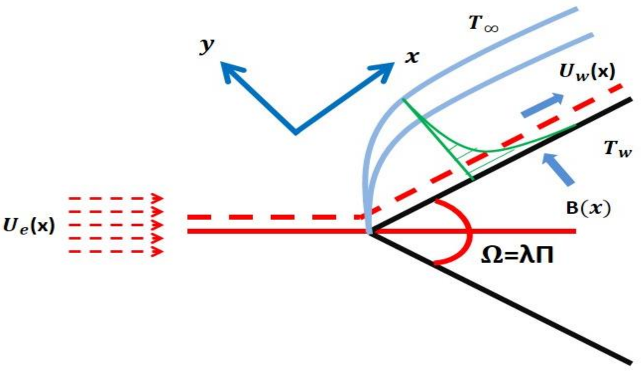

Figure 1: Geometry of the problem.

Consider a two-dimensional, incompressible Carreau fluid past a wedge in the presence of thermal radiation and non-uniform hear source/sink. The coordinate system is chosen such that the x-coordinate is parallel to the surface of the wedge and the y-coordinate is normal to it. It is assumed that the free stream velocity is $u_e(x) = U_\infty x^m$ and the velocity of moving wedge is $u_w(x) = U_w x^m$, where m the Falkner-Skan power-law parameter. T_∞ denotes the ambient fluid temperature and T_w represents the surface temperature. A variable magnetic field

$B(x) = B_0 x^{m-1/2}$ is applied to the flow direction as shown in Fig. 1. The induced magnetic field is neglected in this study. The governing boundary layer equations of flow and heat transfer are as follows [see 31, 32, and 45];

$$\frac{\partial u}{\partial x} + \frac{\partial v}{\partial y} = 0, \tag{1}$$

$$u\frac{\partial u}{\partial x} + v\frac{\partial u}{\partial y} = u_e\frac{\partial u_e}{\partial x} + \nu\left(\frac{\partial^2 u}{\partial y^2} + \frac{3(n-1)}{2}\Gamma^2\left(\frac{\partial u}{\partial y}\right)^2\frac{\partial^2 u}{\partial y^2}\right) - \frac{\sigma B^2}{\rho}(u_e - u) = 0, \tag{2}$$

$$u\frac{\partial T}{\partial x} + v\frac{\partial T}{\partial y} = \alpha\left(\frac{\partial^2 T}{\partial z^2}\right) - \frac{1}{\rho c_p}\frac{\partial q_r}{\partial y} + \frac{1}{\rho c_p}q''' = 0, \tag{3}$$

In which u, v are the velocity components in x, y directions respectively, ν the kinematic viscosity coefficient, Γ the time constant, ρ the density of the fluid, σ the electric conductivity, B the magnetic field, T the temperature.

The radiative heat flux expression is given by;

$$\frac{\partial q_r}{\partial y} = -\frac{16\sigma^*}{3k^*}T_\infty^3\frac{\partial^2 T}{\partial y^2}, \tag{4}$$

The space and temperature dependent heat generation/absorption (non-uniform heat source/sink) q''' are defined as [18]

$$q''' = \left(\frac{k u_w(x)}{x\nu}\right)\left(A^*(T_w - T_\infty)f' + B^*(T - T_\infty)\right), \tag{5}$$

where σ^* and k^* are the Stefan-Boltzman constant and the mean absorption coefficient respectively, where A^* and B^* are parameters of the space and temperature dependent internal heat generation/absorption.

The corresponding boundary conditions are given by;

$$u = u_w, \quad v = 0, \quad T = T_w, \text{ at } \quad y = 0,$$

$$u \to u_e, \quad T \to T_\infty, \quad \text{as} \quad z \to \infty, \tag{6}$$

Now introduce stretching transformations

$$\eta = \sqrt{\frac{(1+m)u_e}{2\nu x}}\, y, \qquad v = -\sqrt{\frac{(1+m)}{2}}\sqrt{\frac{\nu u_e}{x}}\left(f(\eta) + \frac{n-1}{n+1}\eta f'(\eta)\right)$$

$$\theta = \frac{k(T - T_\infty)}{q_w}\sqrt{\frac{(1+m)u_e}{2\nu x}}, \quad u = axf'(\eta), \tag{7}$$

in to Eqns. (2) to (6). One can we have;

$$f''' + ff'' + \frac{2m}{m+1}(1 - f'^2) + \frac{3(n-1)}{2}We f''^2 f''' - M(f' - 1) = 0, \tag{8}$$

$$\frac{1}{Pr}\left(1 + \frac{4}{3}R\right)\theta'' + f\theta' + \frac{m-1}{m+1}f'\theta + A^* f' + B^*\theta = 0 \tag{9}$$

The transformed boundary conditions are as follows;

$$f(\eta) = 0, f'(\eta) = \lambda, \theta(\eta) = 1 \text{ at } \eta = 0,$$

$$f'(\eta) \to 1, \theta(\eta) \to 0 \text{ as } \eta \to \infty \tag{10}$$

here M - magnetic parameter, W_e - Weissenberg number, n -power law index parameter, m -Falkner-Skan power-law parameter Pr -Prandtl number, R - thermal radiation parameter, A^* and B^* are non-uniform heat source/sink parameters, Re_x -local Reynolds number. It is worth to mention that, $\lambda > 0$ corresponds to a stretching wedge, $\lambda < 0$ corresponds to a shrinking wedge and $\lambda = 0$ corresponds to a fixed wedge.which are given by

$$M = \frac{\sigma B_0^2}{\rho b}, We = \frac{\Gamma^2 x^2 b^3}{\nu}, \lambda = \frac{U_w}{U_\infty}, \gamma = \frac{2m}{m+1},$$

$$Re_x = \frac{u_w x}{\nu}, Pr = \frac{\mu c_p}{\rho}, R = \frac{16\sigma^* T_\infty^3}{3k^* k}, \quad (11)$$

The friction factor coefficients and local Nusselt are given by;

$$C_f \left[\frac{2Re_x}{m+1}\right]^{1/2} = \left[f''(0) + \frac{(n-1)We}{2}\left(f''(0)\right)^3\right], \quad (12)$$

$$Nu_x \left[\frac{(m+1)Re_x}{2}\right]^{-1/2} = -\left(1 + \frac{4}{3}R\right)\theta'(0), \quad (13)$$

RESULTS AND DISCUSSION

This section provides a physical interpretation of the key parameters involved in the problem. The effects of the magnetic parameter (M), wedge parameter (λ), Weissenberg number (W_e), power-law index (n), Falkner-Skan power-law parameter (m), Prandtl number (Pr), heat source/sink parameters (A^*, B^*), and radiation parameter (R) on the velocity field $f'(\eta)$ and temperature profile $\theta(\eta)$ are illustrated in Fig. 2 to 12. Additionally, the validation results are compared and presented in Tables 1 and 2. Furthermore, the benchmark results, along with the variations in the skin friction coefficient and Nusselt number, are summarized in Table 3. Figures 2 and 3 illustrate the impact of the magnetic field parameter on the velocity and temperature fields of Carreau fluid. The results indicate that an increase in the magnetic field parameter enhances the velocity field while decreasing the temperature field. This behaviour can be attributed to the reduced dominance of retarding forces in the flow. Similarly, Figures 4 and 5 depict the influence of the parameter γ on the velocity and temperature fields. An increase in γ improves the velocity field and lowers the temperature field, likely for the same reason of diminished retarding forces.

Figure 6 illustrates the effect of the parameter λ on the velocity profile $f'(\eta)$. An increase in λ (defined as $\lambda = U_w/U_\infty$) enhances the velocity at the wall, thereby accelerating the fluid motion. As a result, the velocity profile rises with higher values of the stretching wedge parameter. Conversely, Figure 7 presents the influence of λ on the temperature profile $\theta(\eta)$ for a stretching wedge ($\lambda > 0$). Unlike the velocity profile, the temperature profile exhibits a decreasing trend with increasing values of λ, indicating an inverse qualitative relationship between the velocity and temperature profiles. Fig. 8 illustrates the temperature field profiles for various values of the radiation parameter (R). The results indicate that higher values of the radiation parameter lead to an increase in both the temperature and the thickness of the associated thermal boundary layer. Physically, this occurs because enhanced radiation transfers more heat to the working fluid, thereby thickening the thermal boundary layer. The influence of the Prandtl number (Pr) on the temperature profile $\theta(\eta)$ is depicted in Fig. 9. It is evident that an increase in Pr results in a reduction in the thermal boundary layer thickness. This behaviour is attributed to the dependence of the Prandtl number on thermal diffusivity, where higher Pr values indicate lower thermal diffusivity, reducing heat transfer within the fluid and thereby thinning the thermal boundary layer.

Figures 10 to 12 illustrate the variation of the temperature profile $\theta(\eta)$ for different values of (n), (A^*), and (B^*), respectively. The influence of n, A^*, and B^* is found to enhance the temperature field and the corresponding boundary layer thickness. This can be attributed to the heat source contributing additional heat to the moving wedge, thereby raising its temperature and promoting fluid flow within the boundary layer. Tables 1 and 2 present the validation of the friction factor coefficient and local Nusselt number for varying values of m and Pr. The current results have been compared with the findings of Yacob et al. [24] and Kuo [22], demonstrating excellent agreement, which confirms the accuracy of the present analysis. Numerical values of the friction factor coefficient and local Nusselt number for both the stretching wedge ($\lambda > 0$) and shrinking wedge ($\lambda < 0$) cases are provided in Table 3. It is observed that an increase in the parameters M and n leads to a higher drag force, whereas W_e exhibits an opposite trend in both cases. The rate of heat transfer improves with an increase in $Pr, R,$ and W_e, while a decrease is noted for A^*, B^*, and n in both stretching and shrinking wedge scenarios.

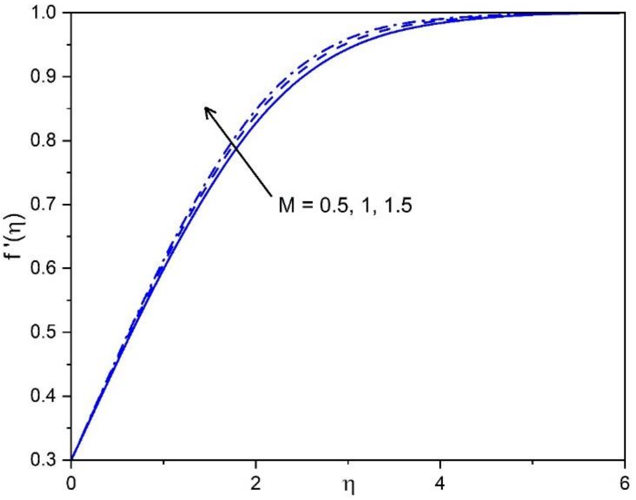

Fig 2: Velocity profiles for different values of M.

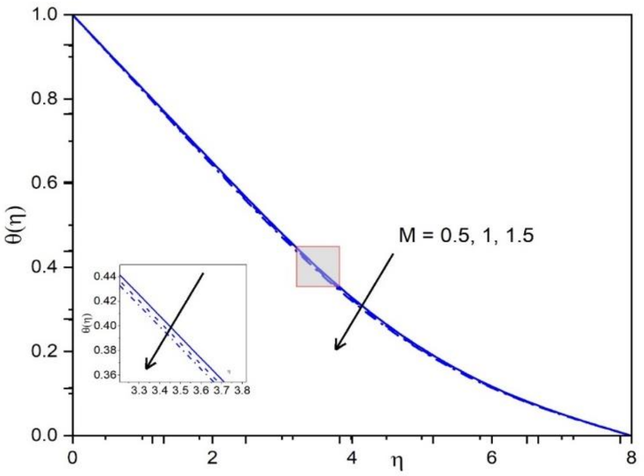

Fig 3: Temperature profiles for different values of M.

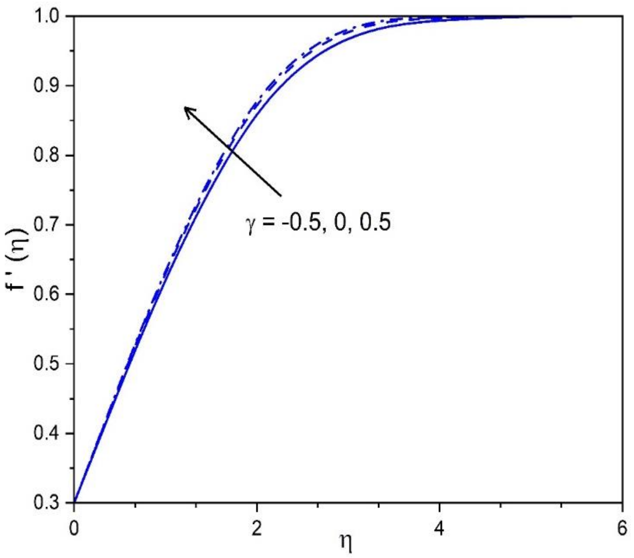

Fig 4: Velocity profiles for different values of γ.

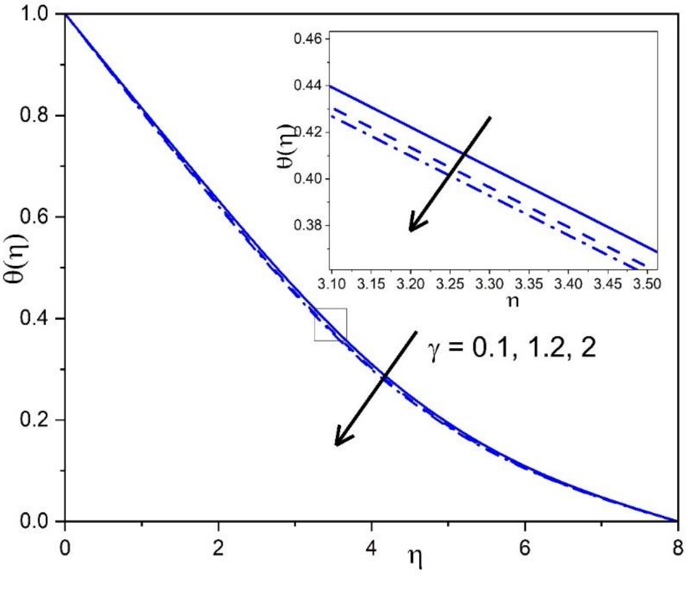

Fig 5: Temperature profiles for different values of γ.

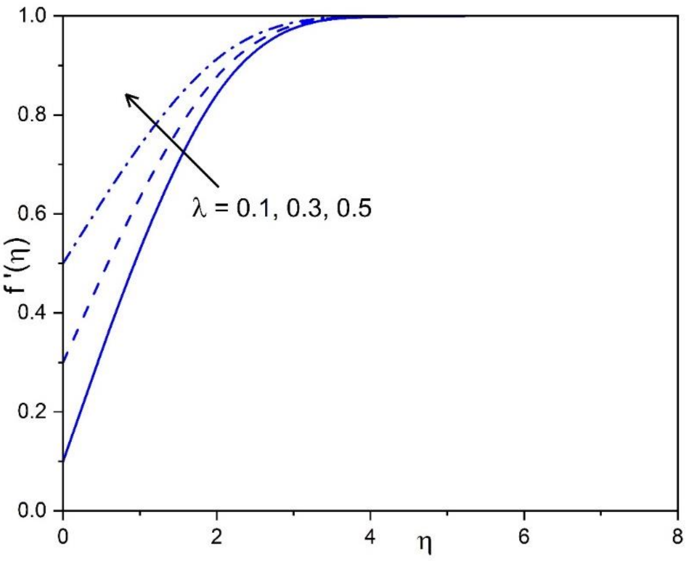

Fig 6: Velocity profiles for different values of λ.

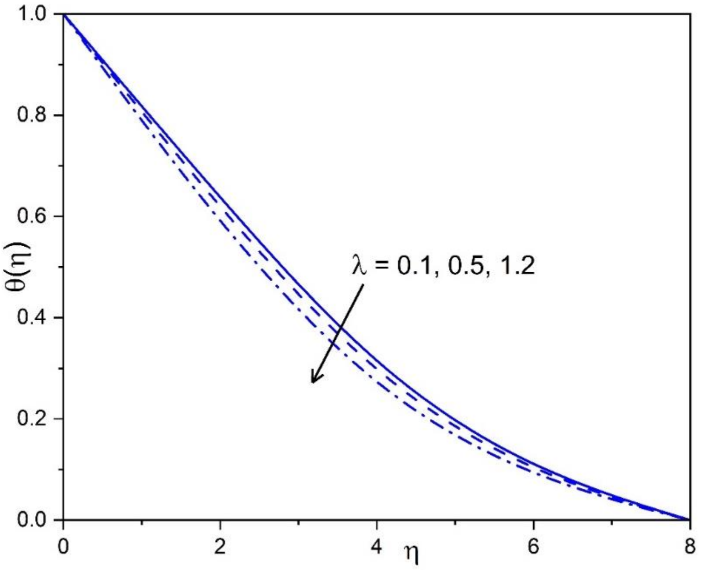

Fig 7: Temperature profiles for different values of λ.

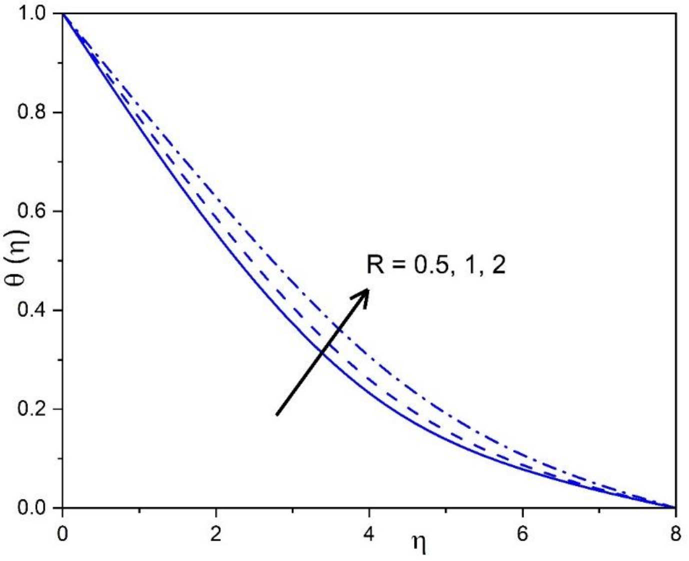

Fig 8: Temperature profiles for different values of R.

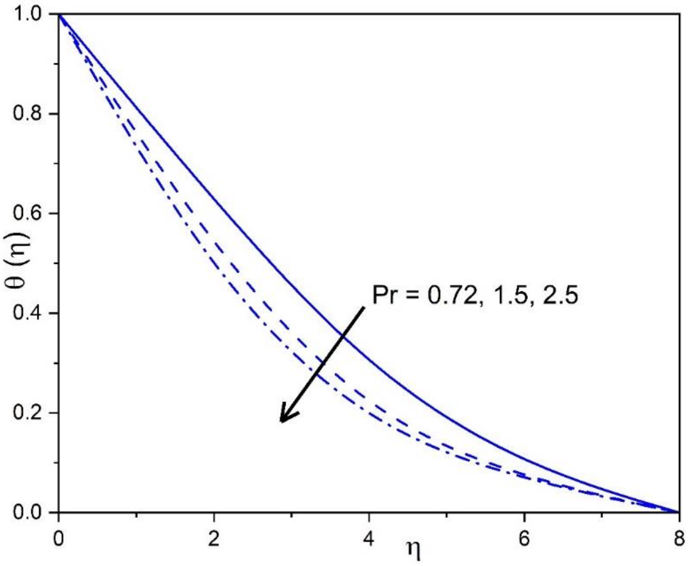

Fig 9: Temperature profiles for different values of Pr.

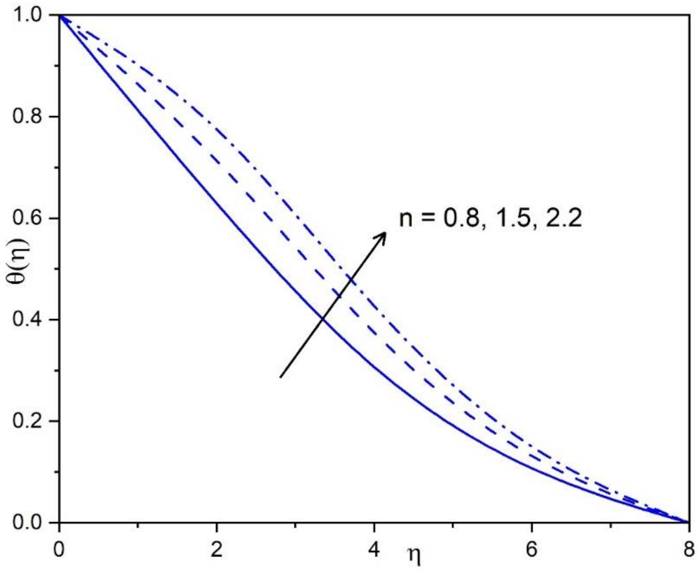

Fig 10: Temperature profiles for different values of n.

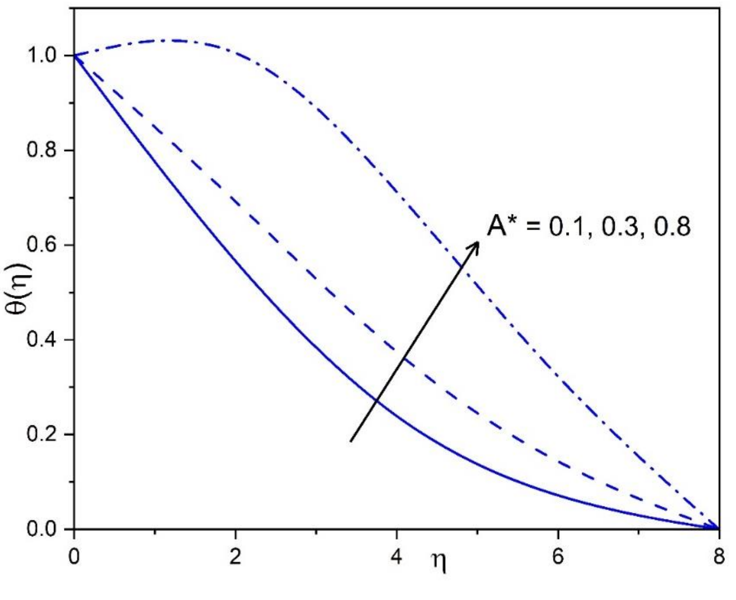

Fig 11: Temperature profiles for different values of A^*.

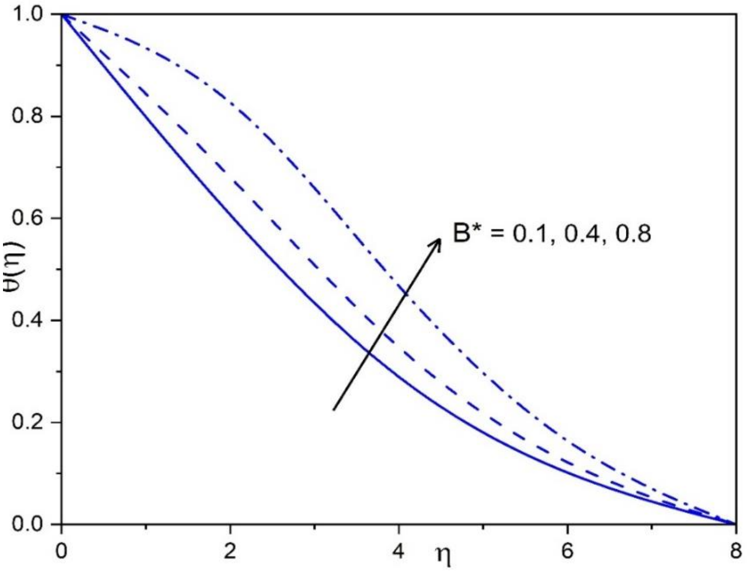

Fig 12: Temperature profiles for different values of B^*.

Table 1: Comparison of skin friction values $f''(0)$ for various values of m with $Pr = 0.72$ and $A^* = B^* = M = R = \lambda = W_e = 0$.

m	Yacob et al. [24]	Present results
0	0.4696	0.469600
1/11	0.6550	0.654994
1/5	0.8021	0.802126
1/3	0.9277	0.927680
1/2	-	1.038903
1	1.2326	1.232588

Table 2: Comparison of local Nusselt number values for various values of Pr with $A^* = B^* = M = R = W_e = 0, n = 1$.

Pr	$\lambda = 0$		$\lambda = 2$	
	Kuo [22]	Present results	Kuo [22]	Present results
0.72	0.41809	0.418091	0.5298	0.529608
1.0	0.46960	0.46960	0.60541	0.605197
10	1.02974	1.029747	1.4561	1.45575
30	1.4873	1.487319	2.1582	2.157737
100	2.2229	2.222906	3.2869	3.28625

Table 3: Numerical values of $C_{fx}Re_x^{\frac{1}{2}}$ and $Re_x^{-\frac{1}{2}}Nu_x$ for various physical parameters.

A^*	B^*	M	Pr	R	λ	W_e	n	$\lambda = 0.5$		$\lambda = -0.5$	
								$C_{fx}Re_x^{\frac{1}{2}}$	$Re_x^{-\frac{1}{2}}Nu_x$	$C_{fx}Re_x^{\frac{1}{2}}$	$Re_x^{-\frac{1}{2}}Nu_x$
0.2	0.2	1.5	0.72	2	0.3	0.5	0.8	1.099131	0.608745	0.70882	0.572851
0.5								1.099131	-0.063785	0.70882	-0.072064
0.8								1.099131	-0.736315	0.70882	-0.71698
	0.2							1.099131	0.608745	0.70882	0.572851
	0.5							1.099131	-0.175922	0.70882	-0.126904
	0.8							1.099131	-0.398333	0.70882	-0.472314
		0.5						0.866367	0.591899	0.249189	0.505403
		1						0.990262	0.601339	0.522876	0.550543
		1.5						1.099131	0.608745	0.70882	0.572851
			0.72					1.099131	0.608745	0.70882	0.572851
			2					1.099131	0.68323	0.70882	0.608177
			4					1.099131	0.646878	0.70882	0.528284
				0.5				1.099131	0.306813	0.70882	0.277738
				1				1.099131	0.41489	0.70882	0.382805
				2				1.099131	0.608745	0.70882	0.572851
					0.3			1.099131	0.608745	0.70882	0.572851

					0.5			0.812993	0.638335	0.511339	0.61375
					0.8			0.340115	0.681969	0.207434	0.672656
						0.1		1.115111	0.607289	0.712984	0.572119
						0.5		1.099131	0.608745	0.70882	0.572851
						1		1.074948	0.610991	0.703305	0.573828
							0.8	1.099131	0.608745	0.70882	0.572851
							1.5	1.158217	0.227715	0.725776	0.208257
							2	1.189906	0.028131	0.736312	0.01.531

Concluding Remarks

Radiative heat transfer in Falkner-Skan flow of a Carreau fluid over a wedge with non-uniform heat source/sink and magnetic field are explored. The reduced system of nonlinear ordinary differential equations (ODE's) are numerically solved using the shooting method, yielding detailed insights into the velocity and temperature distributions. The key findings are;

- The magnetic field parameter plays a crucial role in influencing both the heat transfer rate and the friction factor coefficients.
- The wedge parameter (λ) has a pronounced and favourable effect on the Falkner-Skan flow, enhancing fluid motion.
- The temperature gradient and thermal boundary layer thickness near the wedge decrease due to the effects of $M, \lambda,$ and γ.
- Thermal radiation and heat generation significantly increase the temperature distribution in the fluid.
- Higher values of the Weissenberg number (W_e) enhance the heat transfer rate while reducing the friction factor coefficients.

REFERENCE

1. P.J. Carreau, "Rheological equations from molecular network theories." Transactions of the Society of Rheology 16, no. 1 (1972): 99-127.
2. D. Corradini, "Buffer additives other than the surfactant sodium dodecyl sulfate for protein separations by capillary electrophoresis." Journal of Chromatography B: Biomedical Sciences and Applications 699, no. 1-2 (1997): 221-256.
3. C. Heller, "Principles of DNA separation with capillary electrophoresis." Electrophoresis 22, no. 4 (2001): 629-643.
4. M.R. Davidson, R.P. Bharti, and Dalton JE Harvie. "Electro viscous effects in a Carreau liquid flowing through a cylindrical microfluidic contraction." Chemical engineering science 65, no. 23 (2010): 6259-6269.
5. K. Vajravelu, S. Sreenadh, and R. Saravana. "Combined influence of velocity slip, temperature and concentration jump conditions on MHD peristaltic transport of a Carreau fluid in a non-uniform channel." Applied Mathematics and Computation 225 (2013): 656-676.
6. A.S. Dogonchi, K. Divsalar, and D. D. Ganji. "Flow and heat transfer of MHD nanofluid between parallel plates in the presence of thermal radiation." Computer Methods in Applied Mechanics and Engineering 310 (2016): 58-76.

7. C.S.K. Raju, and N. Sandeep. "Falkner-Skan flow of a magnetic-Carreau fluid past a wedge in the presence of cross diffusion effects." The European Physical Journal Plus 131 (2016): 1-13.
8. B.J. Gireesha, P.B. Sampath Kumar, B. Mahanthesh, S.A. Shehzad, and A. Rauf. "Nonlinear 3D flow of Casson-Carreau fluids with homogeneous–heterogeneous reactions: a comparative study." Results in physics 7 (2017): 2762-2770.
9. K. Ur Rehman, A.S. Alshomrani, and M. Y. Malik. "Carreau fluid flow in a thermally stratified medium with heat generation/absorption effects." Case studies in thermal engineering 12 (2018): 16-25.
10. G.R. Machireddy, and N. Sandeep, "Heat and mass transfer in radiative MHD Carreau fluid with cross diffusion." Ain Shams Engineering Journal 9, no. 4 (2018): 1189-1204.
11. M. Madhu, B. Mahanthesh, N.S. Shashikumar, S.A. Shehzad, S.U. Khan, and B.J. Gireesha. "Performance of second law in Carreau fluid flow by an inclined microchannel with radiative heated convective condition." International Communications in Heat and Mass Transfer 117 (2020): 104761.
12. W.F. Alfwzan, F.M. Allehiany, A. Riaz, S. Sikandar, and G. Alhamzi. "Mathematical model of ciliary flow and entropy for carreau nanofluid with electroosmosis and radiations in porous medium: a numerical work." Case Studies in Thermal Engineering 49 (2023): 103230.
13. M.H. Shahzad, A. Ullah Awan, A. Akgül, S. Nadeem, K. Guedri, M. K.Hassani, and B. M. Makhdoum. "Analytical investigation of Carreau fluid flow through a non-circular conduit with wavy wall." Scientific Reports 14, no. 1 (2024): 2437.
14. M.D. Kumar, P. Jayasri, José Luis Díaz Palencia, P. Durgaprasad, Ali J. Chamkha, and C. S. K. Raju. "Analysis of biomagnetic blood Carreau hybrid nanofluid flow in stenotic arteries with motile gyrotactic microorganisms: Response surface optimisation." The European Physical Journal Plus 139, no. 9 (2024): 1-22.
15. K.S. Srinivasa Babu, A. Parandhama, and R. B. Vijaya. "Non-linear MHD convective flow of Carreau nanofluid over an exponentially stretching surface with activation energy and viscous dissipation." SN Applied Sciences 3, no. 3 (2021): 382.and Mechanics/Zeitschrift für Angewandte Mathematik und Mechanik 104, no. 2 (2024): e202300100.
16. V. M. Falkner and S. W. Skan, "Some approximate solutions of the boundary-layer equations," Philosophical Magazine, 12 (1931) 865–896.
17. D. R. Hartree, "On an equation occurring in Falkner and Skan's approximate treatment of the equations of the boundary layer," Mathematical Proceedings of the Cambridge Philosophical Society, 33(2) (1937) 223–239.
18. K. Stewartson, "Further solutions of the Falkner-Skan equation," Math. Pro. Cambridge Philosophical Soc., 50 (1954) 454–465.
19. K. K. Chen and P. A. Libby, "Boundary layers with small departure from the Falkner-Skan profile," Journal of Fluid Mechanics, 33(2) (1968) 273–282.
20. E. F. F. Botta, F. J. Hut, and A. E. P. Veldman, "The role of periodic solutions in the Falkner- Skan problem for $\lambda > 0$," J. Eng. Math., 20(1) (1986) 81–93.
21. P. Brodie and W. H. H. Banks, "Further properties of the Falkner-Skan equation", Acta Mechanica, 65(1-4) (1987) 205–211.
22. B. L. Kuo, "Application of the differential transformation method to the solutions of Falkner-Skan wedge flow", Acta Mechanica, 164(3-4) (2003) 161–174.
23. Ishak, R. Nazar, I. Pop, "MHD boundary layer flow past a moving wedge", Magnetohydrodynamics, **45** (2009) 3-10.
24. N.A. Yacob, A. Ishak and I. Pop, "Falkner–Skan problem for a static or moving wedge in nanofluids", Int. J. Therm. Sci., 50(2) (2011) 133–139.
25. N.A. Yacob, A. Ishak, R. Nazar and I. Pop, "Falkner–Skan problem for a static and moving wedge with prescribed surface heat flux in a nanofluid", Int. Commun. Heat Mass Transf., 38(2) (2011) 149–153.
26. O. D. Makinde, "Similarity solution for natural convection from a moving vertical plate with internal heat generation and a convective boundary condition" Thermal Science, 15 (2011), Suppl. 1, S137-S143.
27. M. M. Rashidi, M. Ali, N. Freidoonimehr, B. Rostami, M. Anwar Hossain. "Mixed convective heat transfer for MHD viscoelastic fluid flow over a porous wedge with thermal radiation", Advances in Mech. Eng., 6 (2014) 735939.
28. M. Turkyilmazoglu, "Extending the traditional Jeffery-Hamel flow to stretchable convergent/divergent channels", Computers & Fluids, 100 (2014) 196-203.

29. S. Abbasbandy, T. Hayat, A. Alsaedi, M. M. Rashidi. “Numerical and analytical solutions for Falkner-Skan flow of MHD Oldroyd-B fluid”, Int. J. Num. Meth. Heat & Fluid Flow 24(2) (2014) 390-401.
30. M. Turkyilmazoglu, “Slip flow and heat transfer over a specific wedge: an exactly solvable Falkner–Skan equation”, J. Eng. Math., 92 (2015) 73–81.
31. T. Hayat, Tasawar, Sumaira Qayyum, Maria Imtiaz, and Ahmed Alsaedi. "Radiative Falkner-Skan flow of Walter-B fluid with prescribed surface heat flux." Journal of Theoretical and Applied Mechanics 55, no. 1 (2017): 117-127.
32. H.T. Basha, R. Sivaraj, A. Subramanyam Reddy, Ali J. Chamkha, and M. Tilioua. "Impacts of temperature-dependent viscosity and variable Prandtl number on forced convective Falkner–Skan flow of Williamson nanofluid." SN Applied Sciences 2 (2020): 1-14.
33. A.Y. Bakier, “Thermal radiation effect on mixed convection from vertical surface in saturated porous media”, Int. Commun. Heat Mass Transf., 28(1) (2001) 119–126.
34. M. Q. Al-Odat, F. M. S. Al-Hussien and R. A. Damseh, “Influence of radiation on mixed convection over a wedge in non-Darcy porous medium”, Forschung im Ingenieurwesen, 69 (2005) 209–215.
35. O. D. Makinde, “Chemically reacting hydromagnetic unsteady flow of a radiating fluid past a vertical plate with constant heat flux”, Zeitschrift fur Naturforschung, 67a (2012) 239-247.
36. M. Turkyilmazoglu and I. Pop, “Heat and mass transfer of unsteady natural convection flow of some nanofluids past a vertical infinite flat plate with radiation effect,” Int. J. Heat Mass Transfer59, 167-171 (2013).
37. D. Pal and H. Mondal, “Influence of temperature-dependent viscosity and thermal radiation on MHD forced convection over a non-isothermal wedge,” App. Math. and Computation, 212(1) (2009) 194–208.
38. B. J. Gireesha and B. Mahanthesh, “Perturbation solution for radiating viscoelastic fluid flow and heat transfer with convective boundary condition in nonuniform channel with hall current and chemical reaction” , ISRN Thermodynamics (2013) 14 pages, http://dx.doi.org/10.1155/2013/935481.
39. Mushtaq, M. Mustafa, T. Hayat and A. Alsaedi, “Nonlinear radiative heat transfer in the flow of nanofluid due to solar energy: A numerical study”, Journal of the Taiwan Inst. Chem. Eng., 45(4) (2014) 1176-1183.
40. S. A. Shehzad, T. Hayat, A. Alsaedi and M. A. Obid, “Nonlinear thermal radiation in three-dimensional flow of Jeffrey nanofluid: A model for solar energy”, App. Math. And Computation, 248 (2014) 273-286.
41. T. Hayat, M. Imtiaz A, Alsaedi and M. A. Kutbi, “MHD three-dimensional flow of nanofluid with velocity slip and nonlinear thermal radiation”, J. Magnetism and Magnetic Materials, 396 (2015) 31-37.
42. B. Mahanthesh, B.J. Gireesha and R. S. R. Gorla, “Nonlinear radiative heat transfer in MHD three-dimensional flow of water based nanofluid over a non-linearly stretching sheet with convective boundary condition”, J. Nigerian Math. Soc., 35 (2016) 178–198.
43. K. R. Rajagopal, A. S. Gupta, T.Y. Nath, “A note on the Falkner-Skan flows of a non-Newtonian fluid”, Int. J. Non-Linear Mech., 18 (1983) 313-320.
44. Ullah, I. Khan, S. Shafie, “Hydromagnetic Falkner - Skan flow of Casson fluid past a moving wedge with heat transfer” Alexandria Engineering Journal, 55 (2016) 2139–2148.
45. N. Sandeep, and C. Sulochana. "Momentum and heat transfer behaviour of Jeffrey, Maxwell and Oldroyd-B nanofluids past a stretching surface with non-uniform heat source/sink." Ain Shams Engineering Journal 9, no. 4 (2018): 517-524.